


RESEARCH

Open Access



Epigallocatechin-3-gallate protects bovine ruminal epithelial cells against lipopolysaccharide-induced inflammatory damage by activating autophagy

Wanli Zhao¹, Taiyu Shen¹ , Bichen Zhao¹, Moli Li¹, Zhaoju Deng¹, Yihui Huo¹, Ben Aernouts², Juan J. Loor³, Androniki Psifidi⁴ and Chuang Xu^{1*}

Abstract

Background Subacute ruminal acidosis (SARA) causes an increase in endotoxin, which can induce immune and inflammatory responses in the ruminal epithelium of dairy cows. In non-ruminants, epigallocatechin-3-gallate (EGCG), a major bioactive ingredient of green tea, is well-known to alleviate inflammation. Whether EGCG confers protection against SARA-induced inflammation and the underlying mechanisms are unknown.

Results In vivo, eight ruminally cannulated Holstein cows in mid-lactation were randomly assigned to either a low-concentrate (40%) diet (CON) or a high-concentrate (60%) diet (HC) for 3 weeks to induce SARA ($n=4$). Cows with SARA had greater serum concentrations of tumor necrosis factor (TNF)- α and interleukin-6, and epithelium had histological signs of damage. In vitro, immortalized bovine ruminal epithelial cells (BREC) were treated with lipopolysaccharide (LPS) to imitate the inflammatory damage caused by SARA. Our data revealed that BREC treated with 10 $\mu\text{g}/\text{mL}$ LPS for 6 h successfully induce a robust inflammatory response as indicated by increased phosphorylation of I κ B α and nuclear factor kappa-B (NF- κ B) p65. Pre-treatment of BREC with 50 $\mu\text{mol}/\text{L}$ EGCG for 6 h before LPS challenge promoted the degradation of NLR family pyrin domain containing 3 (NLRP3) inflammasome through activation of autophagy, which further repressed activation of NF- κ B pathway targeting Toll-like receptor 4 (TLR4). Analyses also revealed that the EGCG upregulated tight junction (TJ) protein expression upon incubation with LPS.

Conclusions Subacute ruminal acidosis causes ruminal epithelium injury and systemic inflammation in dairy cows. However, the anti-inflammatory effects of EGCG help preserve the integrity of the epithelial barrier through activating autophagy when BREC are exposed to LPS. Thus, EGCG could potentially serve as an effective therapeutic agent for SARA-associated inflammation.

Keywords Bovine ruminal epithelial cell, Epigallocatechin-3-gallate, Inflammation, Subacute ruminal acidosis

*Correspondence:

Chuang Xu

xuchuang@cau.edu.cn

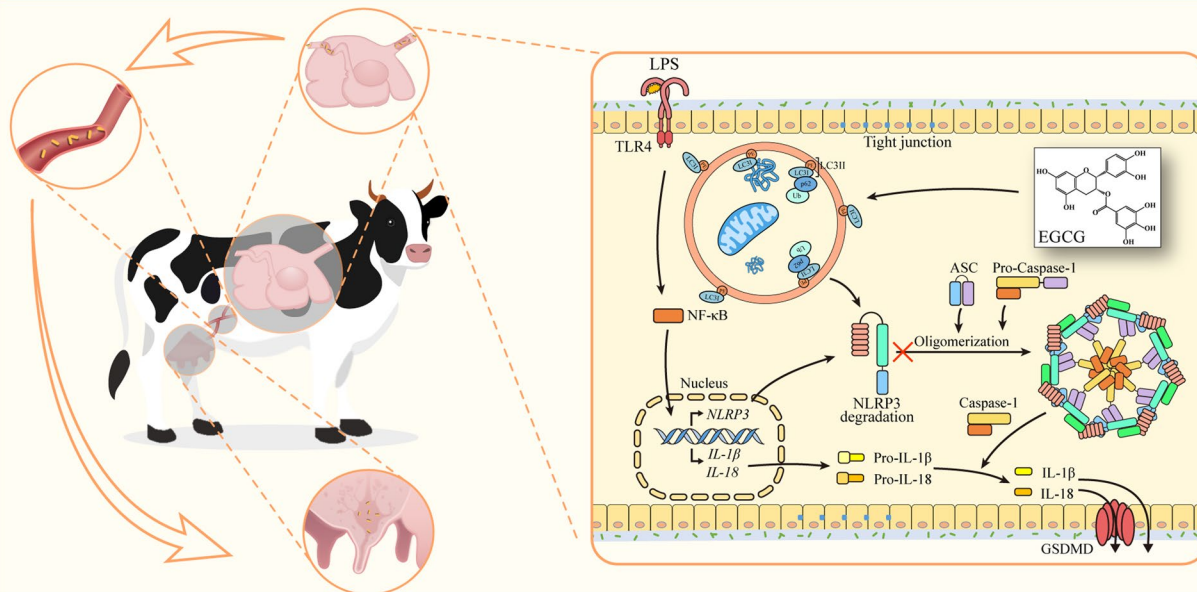
Full list of author information is available at the end of the article



© The Author(s) 2024. **Open Access** This article is licensed under a Creative Commons Attribution 4.0 International License, which permits use, sharing, adaptation, distribution and reproduction in any medium or format, as long as you give appropriate credit to the original author(s) and the source, provide a link to the Creative Commons licence, and indicate if changes were made. The images or other third party material in this article are included in the article's Creative Commons licence, unless indicated otherwise in a credit line to the material. If material is not included in the article's Creative Commons licence and your intended use is not permitted by statutory regulation or exceeds the permitted use, you will need to obtain permission directly from the copyright holder. To view a copy of this licence, visit <http://creativecommons.org/licenses/by/4.0/>. The Creative Commons Public Domain Dedication waiver (<http://creativecommons.org/publicdomain/zero/1.0/>) applies to the data made available in this article, unless otherwise stated in a credit line to the data.

Graphical Abstract

EGCG protects bovine ruminal epithelial cells against LPS-induced inflammation by activating autophagy



Conclusion: Epigallocatechin-3-gallate (EGCG) promotes the degradation of the NLRP3 inflammasome through activating autophagy, reducing NLRP3 inflammasome and caspase-1 production, and thereby inhibiting the LPS/TLR4/NF-κB /NLRP3 axis, eventually attenuating inflammation in LPS-induced bovine ruminal epithelial cell. This is expected to reduce the entry of LPS into the bloodstream through damaged ruminal walls, relieving mammary or systemic inflammatory damage.

Reference: Biasizzo M, Kopitar-Jerala N. Interplay Between NLRP3 Inflammasome and Autophagy. *Front Immunol.* 2020

Background

In an effort to maximize milk production, dairy cows are fed nutrient-dense diets containing a large proportion of cereal grain, thus, increasing susceptibility to disorders such as subacute ruminal acidosis (SARA) and liver abscesses [1, 2]. Excessive intake of highly-fermentable carbohydrates affects the ruminal environment, resulting in lower pH, disturbing flora composition and abundance, and increasing levels of bioactive molecules such as lipopolysaccharides (LPS) [3, 4]. The LPS are located in the cell wall of Gram-negative bacteria, with ruminal acidosis increasing its levels 4-to-16 times compared with normal conditions [5–7]. If uncontrolled, excessive production of LPS can trigger an inflammatory response and cause inflammatory disorders that reduce productivity and cause economic losses [8].

The contact between LPS and its receptor Toll-like receptor 4 (TLR4) activates intracellular signaling through myeloid differentiation primary response protein 88 (MyD88), resulting in the activation of major translocation of nuclear factor kappa-B (NF-κB) [9]. Upon activation of the NF-κB signaling pathway, components linked to inflammasomes are upregulated. Furthermore,

NLRP3 recruits the inflammasome adaptation protein apoptosis-associated speck-like protein containing a CARD (ASC), which then binds and activates caspase-1 [10]. Caspase-1 activation triggers the production of pro-inflammatory cytokines IL-1β and IL-18 [11], which damages the ruminal epithelial barrier and induces systemic inflammation.

Autophagy is an evolutionary conserved intracellular catabolic process that transfers long-lived proteins, misfolded proteins, and excess organelles to the lysosome for degradation [12–14]. Under normal circumstances, autophagy is in a basal state, while it is rapidly upregulated in response to stress factors such as nutrient and energy deficiencies, pathogen-associated molecular patterns (PAMPs) and danger-associated molecular patterns (DAMPs) [15–17]. Autophagy regulates inflammasome activation, including the NLR family pyrin domain containing 3 inflammasome (NLRP3 inflammasome), through multiple mechanisms [18]. The loss of the autophagy-related protein 16-like 1 (ATG16L1) in mouse fetal liver-derived macrophages led to an increase in caspase-1 activation and IL-1β maturation following endotoxin treatment [19]. Furthermore, increasing evidence

revealed an important role of autophagy in the physiology of intestinal epithelial cells including maintenance of barrier function, suggesting that autophagy targeted therapy could be a potential treatment for diseases associated with intestinal barrier dysfunction [20, 21]. Together, available data indicate that activation of autophagy helps control the inflammatory response and maintain proper gastrointestinal barrier integrity. Whether these effects extend to the ruminal epithelial cells (BREC) is unclear.

Green tea possesses multiple physiological and pharmacological benefits, including anti-inflammatory and antioxidant effects, prevention of obesity, diabetes, cancer, and other diseases [22, 23]. The major active ingredient in green tea is epigallocatechin-3-gallate (EGCG), a potent antioxidant that can quench reactive radicals and chelate metal ions to prevent the formation of reactive oxygen species (ROS) [24]. EGCG also has anti-inflammatory effects through blocking the activation of NF- κ B, activator protein-1 (AP-1), MyD88-dependent pathway, Toll-interleukin-1 receptor domain-containing adaptor inducing interferon- β (IFN- β)-dependent pathways of TLR, and the expression of cytochrome c oxidase (COX), nitric oxide (NO) synthase, and TNF- α [25, 26]. EGCG inhibited IL-6, IL-1 β , and TNF- α in LPS-mediated RAW 264.7 cells [27], and induced autophagy, anti-inflammatory responses, degradation of lipid droplets in endothelial cells, and facilitated degradation of endotoxins leading to anti-inflammatory actions [28, 29]. In hepatic cells, EGCG was observed to activate Adenosine 5'-monophosphate (AMP)-activated protein kinase (AMPK), thereby advancing autophagy [30]. EGCG also diminished the effect of negative regulators of autophagy, thereby delaying apoptosis-mediated cell death and extending cell viability [31]. Whether EGCG confers protective effects against LPS-induced inflammatory responses in BREC and the underlying mechanisms are unknown.

We hypothesized that in vivo SARA has a negative effect on the BREC due to the increased release of endotoxins. As such, supplementation of EGCG in vitro would alleviate LPS-induced inflammatory and tight junction (TJ) damage by regulating autophagy. Thus, the objective of this study was to use BREC as an in vitro model when cells were incubated with EGCG and LPS. Several molecular indicators of inflammation, autophagy, and tight junction components were measured in BREC to address our hypothesis.

Materials and methods

Materials

EGCG (HPLC \geq 98%) was purchased from Shanghai yuanye Bio-Technology Co., Ltd. (Shanghai, China). *Escherichia coli* LPS serotype O55:B5 was procured from

Sigma-Aldrich (St. Louis, MO, USA). Chloroquine, a selective inhibitor of autophagy and TLR, was obtained from MCE (MedChemExpress, USA). A stock solution of EGCG was prepared in DMEM/F12 (Hyclone, Logan, UT, USA) medium at concentrations of 1 mmol/L. A stock solution of LPS was prepared in DMEM/F12 medium at a concentration of 1 mg/mL.

Samples

Ruminal tissue epithelia, blood samples from cows with SARA and healthy cows were kindly provided by Dr. Shengyong Mao's group (Nanjing Agricultural University). Data on DMI and ruminal pH of these cows were reported previously [32]. Overall, compared with the CON group, there was no significant difference in DMI due to high-concentrate feeding (23.79 vs. 22.40, $P=0.524$). On average, ruminal pH remained at <5.8 for 9.2 h/d due to high-concentrate feeding. Tissue was collected at slaughter and blood samples prior to sacrifice at the end of their experimental period. Serum inflammatory cytokines were detected via ELISA kits (Lengton, Shanghai, China) according to the manufacturer's instructions. Morphology of ruminal epithelia was identified via microscopy (Olympus, Japan).

Cell culture

Immortalized BREC were provided by Dr. Kang Zhan's group at Yangzhou University [33]. Cells were cultured in DMEM/F12 containing 10% FBS (Gibco, Waltham, MA, USA) and 1% (v/v) penicillin/streptomycin at 37 °C in a humidified incubator with 5% CO₂.

Treatment of BREC

EGCG was diluted with DMEM/F12 to various concentrations (0, 10, 20, 50, 100, 125, 150, 200 and 300 μ mol/L) and used to stimulate BREC for various times (2, 6 and 12 h) to test effects on the viability of BREC. LPS was dissolved in the media at specific concentrations (0, 1, 5 and 10 μ g/mL) and used to stimulate BREC for 6 h to establish the appropriate inflammatory model based on the expression of pro-inflammatory mediators and tight junction proteins using Western blotting. After selecting the concentrations of EGCG and LPS based on cell viability and inflammatory responses, the effect of EGCG (10, 20 and 50 μ mol/L) in LPS-challenged (10 μ g/mL) BREC on the transcription of inflammatory cytokines and chemokines was evaluated. Activation of the NF- κ B pathway targeting TLR4 was investigated using quantitative real-time (qRT)-PCR and Western blotting.

The first experimental treatments were: CON (control; no EGCG pre-treatment, no LPS induction), LPS (no EGCG pre-treatment, 10 μ g/mL LPS induction), E10+LPS (10 μ mol/L EGCG pre-treatment, 10 μ g/mL

LPS induction), E20+LPS (20 $\mu\text{mol/L}$ EGCG pre-treatment, 10 $\mu\text{g/mL}$ LPS induction) and E50+LPS (50 $\mu\text{mol/L}$ EGCG pre-treatment, 10 $\mu\text{g/mL}$ LPS induction). Pre-treatment with EGCG and challenge with LPS each lasted 6 h at 37 °C. Western blotting, qRT-PCR and immunofluorescence were used to evaluate the effect of EGCG (50 $\mu\text{mol/L}$) on autophagy activation and the NLRP3 inflammasome-mediated signaling pathway in LPS-challenged (10 $\mu\text{g/mL}$) BREC.

In second experiment, we compared four groups: CON (control, no EGCG pre-treatment, no LPS induction), LPS (no EGCG pre-treatment, 10 $\mu\text{g/mL}$ LPS induction), EGCG (50 $\mu\text{mol/L}$ EGCG pre-treatment, no LPS induction), and EGCG+LPS (50 $\mu\text{mol/L}$ EGCG pre-treatment, 10 $\mu\text{g/mL}$ LPS induction). In the third experiment, autophagy was inhibited with 50 $\mu\text{mol/L}$ chloroquine (CQ) for 4 h before the EGCG (50 $\mu\text{mol/L}$) pre-treatment and the LPS (10 $\mu\text{g/mL}$) induction. Four groups were compared: LPS, LPS+CQ, EGCG+LPS, and EGCG+LPS+CQ.

Cell viability assay

Cell Counting Kit-8 (CCK-8, Solarbio, Beijing, China) was used to measure cell viability by seeding 1×10^4 cells/well of BREC into 96-well plates for 12 h before treating with different concentrations of EGCG (0, 10, 20, 50, 100, 125, 150, 200 and 300 $\mu\text{mol/L}$) for 2, 6 and 12 h at 37 °C. Subsequently, BREC were washed once with phosphate-buffered solution (PBS), 10 μL of CCK-8 was added to each well, and the BREC incubated at 37 °C for 3 h. An automated microplate reader (Molecular Devices, Shanghai, China) was used to measure the optical density (OD) at 450 nm. Cell viability was calculated as follows: (treatment group OD – blank OD)/(CON group OD – blank OD).

RNA extraction and quantitative real-time PCR

Isolation of total RNA was performed with TRIzol reagent (Vazyme, Nanjing, China). The purity of the RNA was assessed using the A_{260}/A_{280} ratio. The ratio of all samples measured was between 1.8 and 2.0, indicating a high level of purity. The integrity of the RNA was assessed using agarose gel electrophoresis. The extracted RNA sample was 1 μg and mixed with 1 μL of 5 \times RNA Loading Buffer before loading on a 1% agarose gel electrophoresis and run at 100–120 V for 20 min. The integrity of RNA bands was examined using a Tanon gel imaging system (Tanon, Shanghai, China). One μg of total RNA in each sample was reverse-transcribed to cDNA in a 20 μL reaction using a reverse transcription kit (RR047A, TaKaRa Biotechnology Co., Ltd.) according to the supplier's protocol. We evaluated mRNA expression levels using qRT-PCR technology with the SYBR

Green QuantiTect RT-PCR Kit (RR420A; TaKaRa Biotechnology Co., Ltd.) and a 7500 Real-Time PCR System (Applied Biosystems Inc., Waltham, MA, USA). The qRT-PCR was conducted with one cycle of denaturation at 95 °C for 30 s, followed by 40 cycles with denaturation at 95 °C for 5 s and annealing extension at 60 °C for 34 s. The relative quantification values were normalized to the geometric mean of the Cq of the reference genes. Fold-changes in gene expression relative to the mean of each treatment in the control group were calculated using the $2^{-\Delta\Delta\text{CT}}$ method [34]. Every component of a primer pair was located in the target gene's neighboring exons and demonstrated to anneal solely to the target sequence by Primer-BLAST software analysis. Melting curve analysis revealed that amplification with each primer pair produced a single product with efficiencies ranging from 92% to 98%. Data were analyzed by means of a relative standard curve based on serial dilutions of the pooled cDNA prepared from the cell samples. The primer pairs used in this study were designed using Primer Express software (Applied Biosystems Inc.) according to gene sequences published in GeneBank. Primers were manufactured by Sangon Biotech (Shanghai) Co., Ltd. for synthesis. Additional file 1 lists the specific primers and its efficiency values used in the quantitative PCR. Candidate reference genes tested were *ACTB* and *GAPDH*, *ACTB* was used as the internal control for data normalization as it was unaffected by physiological state.

Biochemical analysis

BREC were pre-treated with 50 $\mu\text{mol/L}$ EGCG for 6 h and then challenged with 10 $\mu\text{g/mL}$ LPS for 6 h in 6-well plates (2.5×10^6 cells/mL). Cell-free supernatants were subsequently centrifuged at 3,000 r/min for 20 min and the supernatant used for measuring inflammatory cytokines TNF- α (BPE92091, 4–640 ng/L), IL-6 (BPE92153, 3–480 ng/L) and IL-10 (BPE92159, 4–640 ng/L) via ELISA kits (Lengton, Shanghai, China) according to the manufacturer's instructions. The percentage of caspase-1 activation was detected via the Caspase-1 Activity Assay Kit (Beyotime, Shanghai, China) according to manufacturer's instructions. In brief, cells were harvested at room temperature, and the protein concentration was determined via the Bradford method. A calibration curve was constructed to determine caspase-1 activity.

Western blotting

The Bicinchoninic acid (BCA) kit (Applygen, Beijing, China) was used for determination of protein concentration. Sodium dodecyl sulfate–polyacrylamide gel electrophoresis separation was performed with 30 μg of sample protein per lane and then proteins were transferred to

polyvinylidene fluoride (PVDF) membrane (Pall, Shanghai, China) and blocked with 5% BSA. The blocked membranes were hybridized overnight at 4 °C with antibodies against β -actin (1:100,000; 66009-1-Ig; Proteintech, Wuhan, China), GAPDH (1:50,000; 60004-1-Ig; Proteintech), p-NF- κ Bp65 (1:1,000; bs-0982R; Bioss, Beijing,

China), NF- κ Bp65 (1:1,000; 10745-1-AP; Proteintech), p-I κ B α (1:1,000; MA5-16161; Invitrogen, Beijing, China), I κ B α (1:10,000; 10268-1-AP; Proteintech), Occludin (1:10,000; 27260-1-AP; Proteintech) and ZO-1 (1:10,000; 21773-1-AP; Proteintech), P62(1:1,000; 66184-1-Ig; Proteintech), LC3 (1:1,000; 14600-1-AP; Proteintech), NLRP3

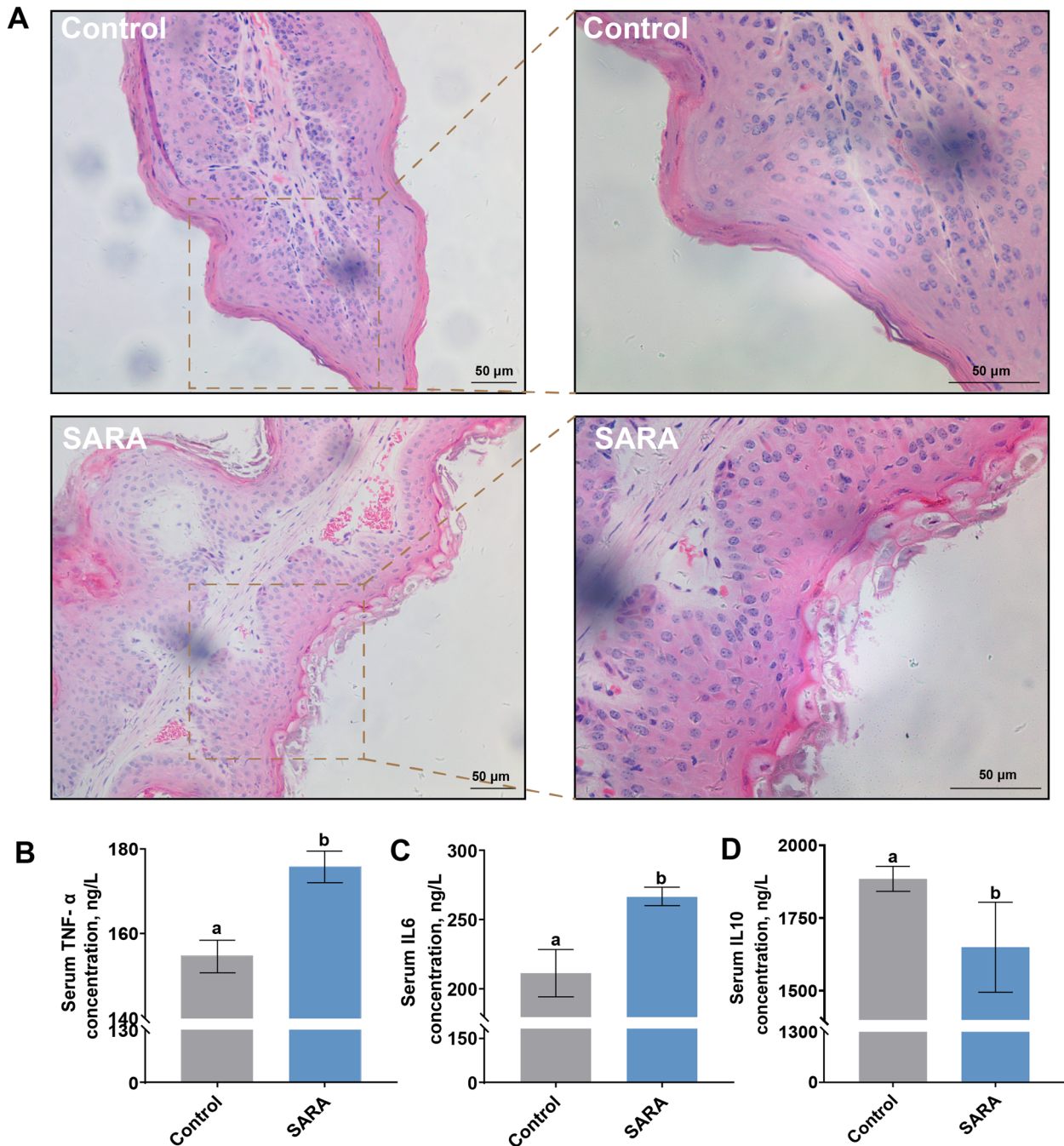


Fig. 1 Ruminal epithelial tissue morphology and serum inflammation biomarkers. **A** H&E of ruminal epithelial tissue. Scale bar = 50 μ m. **B–D** Serum proinflammatory and anti-inflammatory cytokine in dairy cows ($n=4$). ^{a,b}Values without the same letters indicate a significant difference ($P < 0.05$)

(1:10,000; 68102-1-Ig; Proteintech) and caspase-1 (1:1,000; ab179515; Abcam, Cambridge, MA, USA). Then, the membranes were washed and incubated with horse radish peroxidase-conjugated secondary antibody (1:5,000 dilutions in TBST) at room temperature for 45 min. The final blots were developed using enhanced chemiluminescence solution (Abbkine, Wuhan, China) in a Western blotting detection system (Tanon, Shanghai, China). Image J software (National Institutes of Health, Bethesda, MD, USA) was used to measure band intensities.

Immunofluorescence staining

BREC were cultured on a unique detachable chamber of a sterile Nunc Lab-Tek chamber slide system prior to staining. After adhesion, BREC were pre-treated with 50 µmol/L EGCG for 6 h, followed by incubation with 10 µg/mL LPS for 6 h. Then, BREC were fixed with 4% paraformaldehyde for 20 min. After three PBS washes, 5 min each time, the slides were permeabilized for 5 min at 4 °C with 0.2% Triton X-100 in PBS. BREC were blocked for 1 h in 5% goat serum at 4 °C, and incubated with LC3 (1:500; 14600-1-AP; Proteintech), Cytokeratin 18 (1:1,000; 10830-1-AP; Proteintech) overnight at

4 °C. BREC were then washed with PBS, incubated with CoraLite488-conjugated AffiniPure goat anti-rabbit IgG (H+L) in the dark for 1 h, and stained with 500 µL DAPI for 10 min. Immunofluorescence was visualized under a confocal laser-scanning microscope (Leica, Germany). The LC3 average fluorescence intensity were analyzed using Image J software (Mean gray value=Integrated Density/Area).

Statistical analysis

All experiments contained at least three biological replicates. Experimental data between groups were analyzed using GraphPad Prism 8.0 (GraphPad Prism Inc., La Jolla, CA, USA) or SPSS 23.0 software (IBM Corp., Armonk, NY, USA). Data on serum samples from eight cows were normally distributed and analyzed with paired *t*-tests. All other data were normally distributed and analyzed using one-way analysis of variance (ANOVA) followed by Duncan's multiple range test. Data are expressed as mean ± standard error of the mean. Different lowercase letters (a-f) on the bar chart indicate significant differences. Effects were deemed significant when *P* < 0.05.

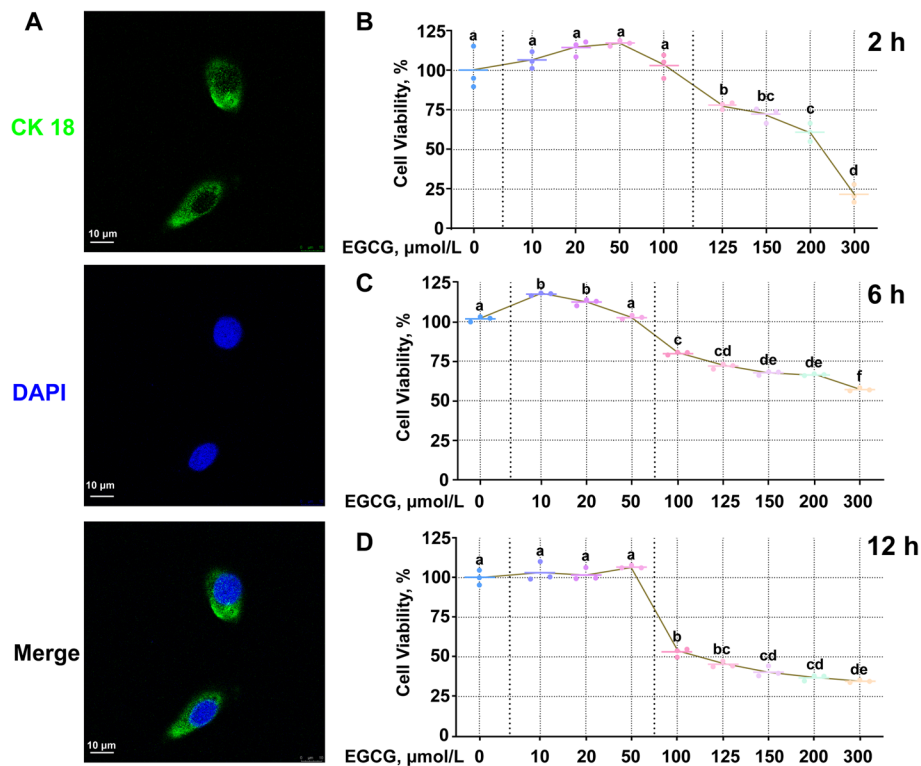


Fig. 2 Identification of bovine ruminal epithelial cells (BREC). **A** Green light denotes Cytokeratin 18 and blue light the nucleus. Scale bar = 10 µm; Cell viability of BREC in response to epigallocatechin-3-gallate (EGCG). **B–D** BREC were treated with various concentrations of EGCG for 2, 6 and 12 h, the first dotted line distinguished the control group from the dosed group and the second dotted line represented a concentration at which the drug significantly reduced cell viability in each graph. ^{a–f}Values without the same letters indicate a significant difference (*P* < 0.05)

Results

Ruminal epithelium histology and blood composition in cows with SARA

Cows with SARA had extensive shedding of the ruminal epithelial papillary stratum corneum and cell death (Fig. 1A). These cows also experienced decreased serum concentrations of the anti-inflammatory cytokine IL-10 along with increased concentrations of the proinflammatory cytokines TNF- α and IL-6 further confirming the injury of epithelial tissue and systemic inflammatory response in cows with SARA (Fig. 1B–D).

Effects of different concentrations of EGCG on bovine ruminal epithelial cell viability

Verification of the epithelial nature of the BREC is illustrated in Fig. 2A. Cell proliferation was not affected by EGCG concentrations equal to or below 100 $\mu\text{mol/L}$, but decreased when above 125 $\mu\text{mol/L}$ EGCG for 2 h ($P < 0.05$, Fig. 2B). Treatment with 10 or 20 $\mu\text{mol/L}$ EGCG for 6 h increased cell proliferation ($P < 0.05$), but for EGCG concentrations equal to or above 100 $\mu\text{mol/L}$ there was a continuous and significant decrease in cell proliferation ($P < 0.05$, Fig. 2C). Cell proliferation was significantly reduced ($P < 0.05$) when BREC were incubated with EGCG concentrations great than or equal to

100 $\mu\text{mol/L}$ for 12 h (Fig. 2D). Based on these findings, 10, 20 and 50 $\mu\text{mol/L}$ EGCG for 6 h were chosen for subsequent studies.

Establishment of optimal inflammatory conditions with LPS

As shown in Fig. 3A–E, increasing LPS concentrations increased phosphorylation of NF- κB p65 and I $\kappa\text{B}\alpha$, with the effect of 10 $\mu\text{g/mL}$ LPS for 6 h being the most significant. Apart from the activation of the NF- κB pathway, the expression of ZO-1 and Occludin proteins also decreased significantly (Fig. 3F–H). Thus, 10 $\mu\text{g/mL}$ LPS treatment for 6 h was chosen as the best model for inducing inflammation in subsequent experiments.

Effect of EGCG on production of inflammatory cytokines and chemokines in LPS-challenged BREC

LPS challenge significantly upregulated the transcription of pro-inflammatory cytokines, including TNF- α , IL-6, IL-1 β (Fig. 4A–C), and the chemokines C-C motif chemokine ligand 2 (CCL2) and C-X-C motif chemokine ligand 14 (CXCL14) (Fig. 4E and F). In contrast, pre-treatment with EGCG for 6 h at high concentrations (50 $\mu\text{mol/L}$) significantly inhibited the transcription of pro-inflammatory

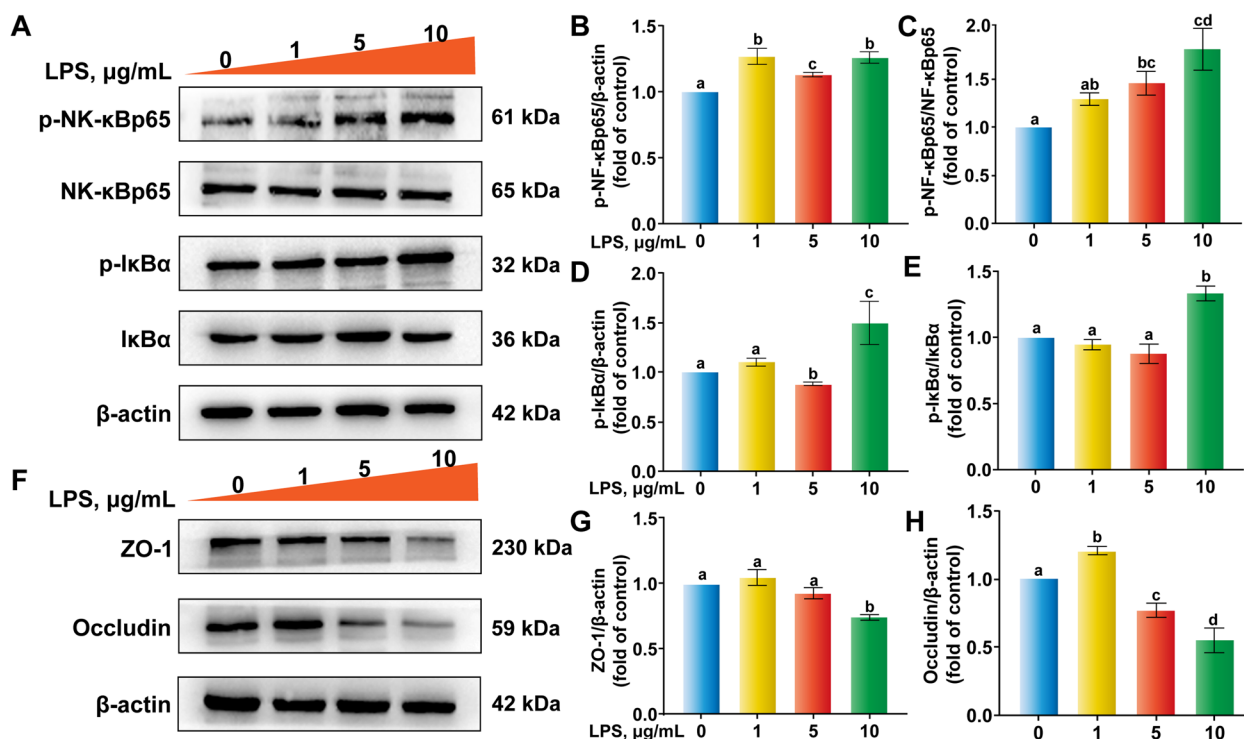


Fig. 3 Pro-inflammatory effect and tight junction protein abundance in response to different concentrations of lipopolysaccharide (LPS) in bovine ruminal epithelial cells. Cells were treated with various concentrations of LPS for 6 h. **A–H** Western blot analysis of the abundance of phosphorylated-nuclear factor kappa-B (p-NF- κB) p65, NF- κB p65, p-I $\kappa\text{B}\alpha$, I $\kappa\text{B}\alpha$, ZO-1 and Occludin. ^{a–d}Values without the same letters indicate a significant difference ($P < 0.05$)

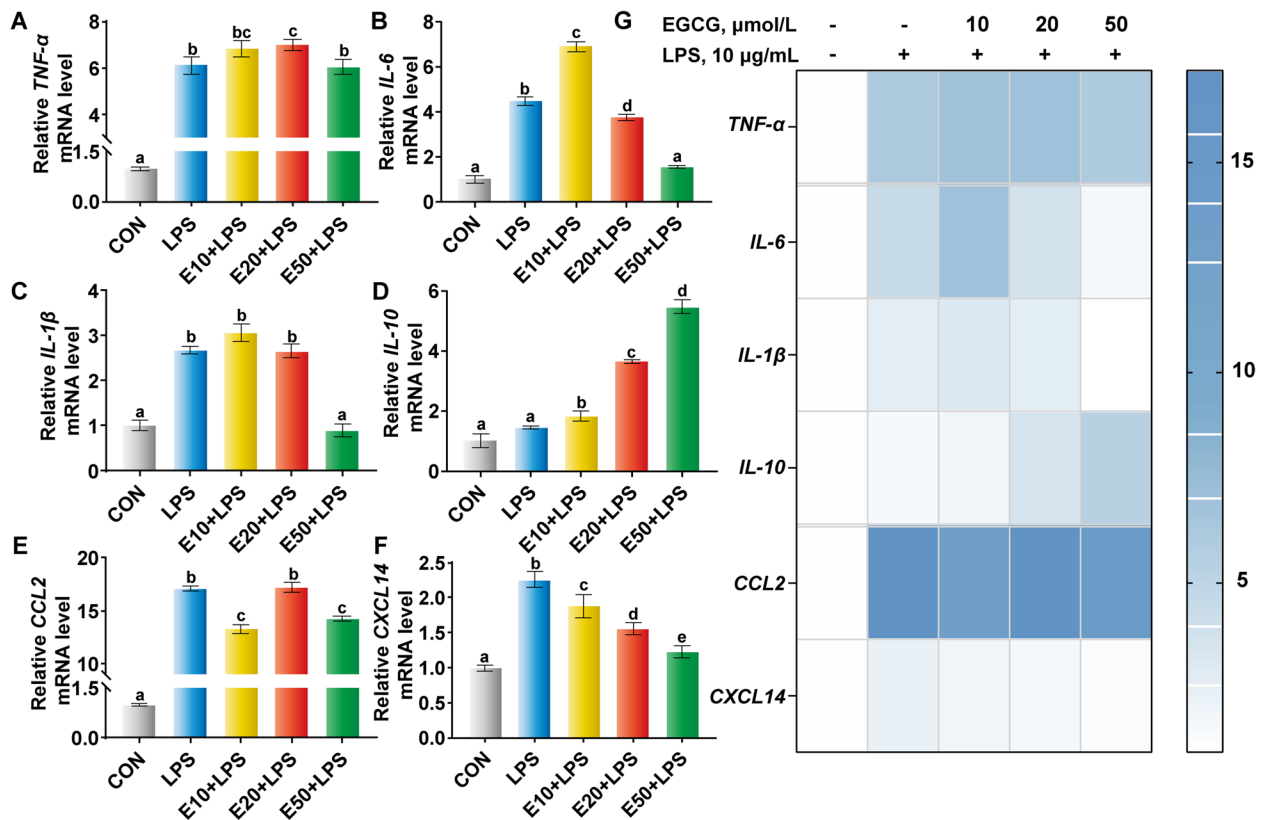


Fig. 4 Effects of different concentrations of epigallocatechin-3-gallate (EGCG) on the production of inflammatory mediators in lipopolysaccharide (LPS)-challenged bovine ruminal epithelial cells. Cells were pre-treated with different concentrations of EGCG (10, 20, or 50 $\mu\text{mol/L}$) for 6 h before being exposed to 10 $\mu\text{g/mL}$ LPS for 6 h in 6-well plates (2.5×10^6 cells/mL). **A–F** The mRNA abundance of tumor necrosis factor (*TNF- α*), *IL-6*, *IL-1 β* , *IL-10*, C-C motif chemokine ligand 2 (*CCL2*) and C-X-C motif chemokine ligand 14 (*CXCL14*). **G** Heat map analysis of the mRNA abundance data. ^{a–d}Values without the same letters indicate a significant difference ($P < 0.05$)

cytokines and up-regulated anti-inflammatory cytokines IL-10 that were induced by LPS (Fig. 4G).

EGCG represses the activation of the NF- κ B pathway targeting TLR4 in LPS-challenged BREC

As evidenced in Fig. 5A–D, LPS exposure significantly upregulated ($P < 0.05$) the mRNA abundance of *TLR4*, *MyD88* and Interleukin 1 receptor associated kinase 1 (*IPAK1*), but pre-treatment with EGCG downregulated these indicators compared with the LPS group ($P < 0.05$). Fifty $\mu\text{mol/L}$ EGCG pre-treatment reversed the upregulated ratio of p-I κ B α to I κ B α and p-NF- κ Bp65 to NF- κ Bp65 in LPS-challenged BREC (Fig. 5E–G). In addition, compared with the LPS group, 50 $\mu\text{mol/L}$ EGCG pre-treatment also restored TJ protein expression of ZO-1 and Occludin (Fig. 5H–J). These results indicated that EGCG exerted anti-inflammatory activity in LPS-challenged BREC, particularly when incubated with 50 $\mu\text{mol/L}$ EGCG for 6 h.

EGCG promotes NLRP3 inflammasome degradation via activating autophagy, a critical aggravator of LPS-challenged systemic damage

Compared with the LPS group, 50 $\mu\text{mol/L}$ EGCG pre-treatment for 6 h upregulated SQSTM1 and downregulated MAP1LC3 transcription (Fig. 6A and B), and significantly reduced NLRP3 inflammasome and cleaved caspase-1 expression at the mRNA abundance level (Fig. 6C and D). In addition, the mRNA abundance of *IL-18* also decreased and the TJ mRNA abundance of *ZO-1*, Occludin and Claudin-1 upregulated due to EGCG pre-treatment in LPS-challenged BREC (Fig. 6E–J).

As shown in Fig. 7A and B, the fluorescence intensity of LPS was lowest among these groups, EGCG pre-treatment activated LC3 further expression. Fifty $\mu\text{mol/L}$ EGCG pre-treatment for 6 h alone had no negative impact on BREC. In contrast, compared with the control group, it decreased caspase-1 activity (Fig. 7C). Within the NLRP3 inflammasome and autophagy activation-mediated signaling pathway, it exerted the decrease in NLRP3 and pro-caspase-1 protein abundance, the

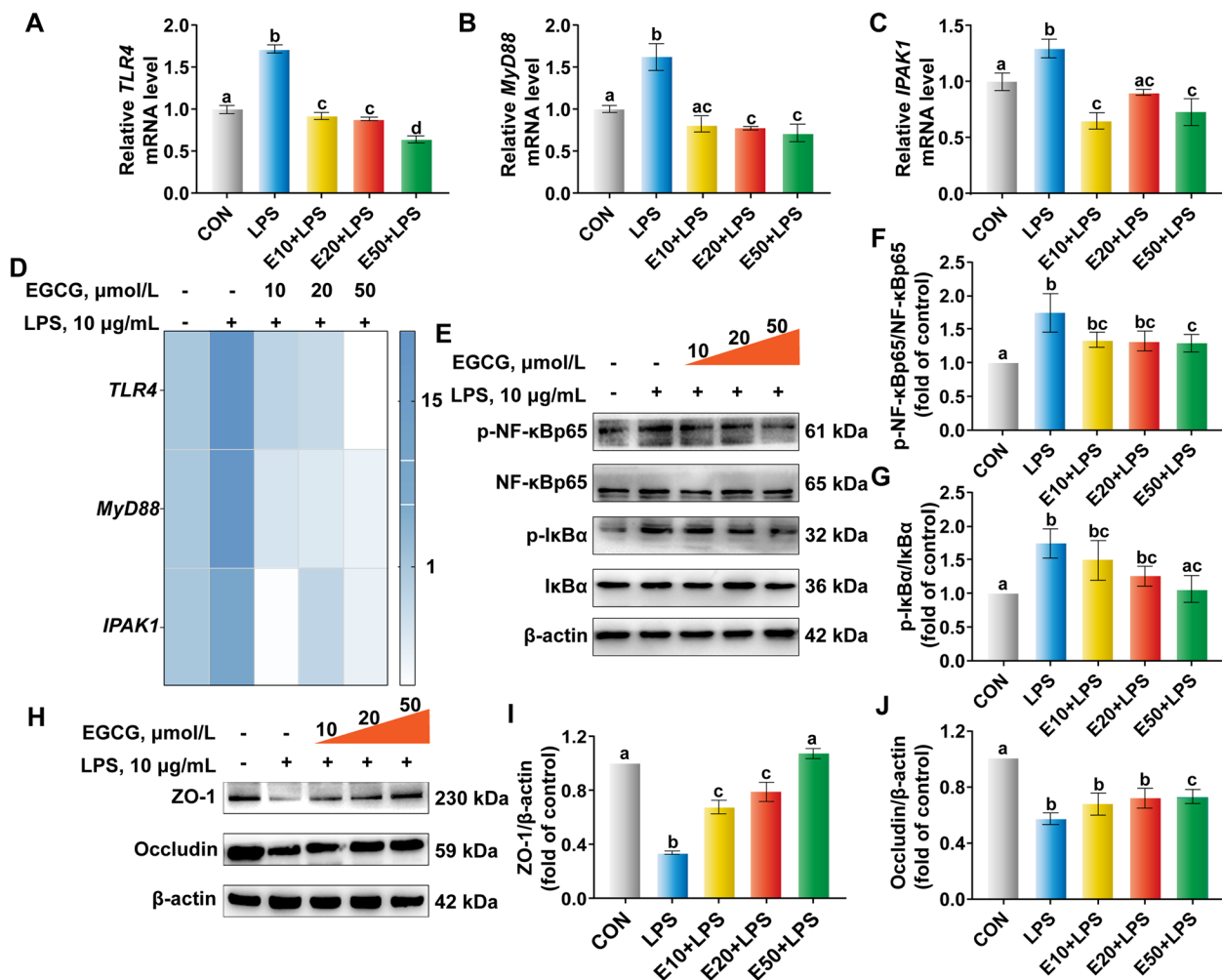


Fig. 5 Effects of different concentrations of epigallocatechin-3-gallate (EGCG) on the nuclear factor kappa-B (NF-κB) pathway targeting Toll-like receptor 4 (TLR4). Cells were preprocessed with different concentrations of EGCG (10, 20, or 50 μmol/L) for 6 h and then added 10 μg/mL lipopolysaccharide (LPS) for 6 h in 6-well plates (2.5×10^6 cells/mL). **A–C** The mRNA abundance of *TLR4*, Myeloid differentiation primary response protein 88 (*MyD88*) and Interleukin 1 receptor associated kinase 1 (*IPAK1*). **D** Heat map analysis of the mRNA abundance. **E–J** Western blot analysis of the abundance of phosphorylated-nuclear factor kappa-B (p-NF-κB p65), NF-κBp65, p-IκBα, IκBα, ZO-1 and Occludin. ^{a–d}Values without the same letters indicate a significant difference ($P < 0.05$)

increased protein abundance of LC3II and the decreased protein abundance of p62 also indicated that EGCG pre-treatment activated autophagy in BREC (Fig. 7E–H). EGCG also decreased markedly the ratio of p-NF-κBp65 to NF-κBp65 and p-IκBα to IκBα, and restored the abundance of TJ proteins under the attack of LPS (Fig. 7I–L).

Compared with EGCG + LPS, the anti-inflammatory cytokine IL-10 decreased significantly and proinflammatory cytokine TNF-α, IL-6 showed rising trend in the CQ+EGCG+LPS (Fig. 8A–C). The mixture of CQ+EGCG+LPS also led to a significant increase in caspase-1 activity and pro-caspase-1 protein abundance, but the NLRP3 inflammasome protein abundance was not significant (Fig. 8D, F and G). The combination with

CQ remarkably reduced LC3II accumulation (Fig. 8I). Compared with EGCG + LPS, Within the NF-κB-related signaling pathway and for TJ protein abundance, CQ pre-treatment reversed the downregulation of protein abundance of the ratio of p-NF-κBp65 to NF-κBp65 and p-IκBα to IκBα in EGCG + LPS, and it also significantly downregulated protein abundance of ZO-1 and Occludin (Fig. 8J–M).

Discussion

Subacute ruminal acidosis has emerged as one of the main metabolic disorders in high-producing dairy cattle affecting milk production, health and welfare. The onset and duration of SARA often leads to destruction of the

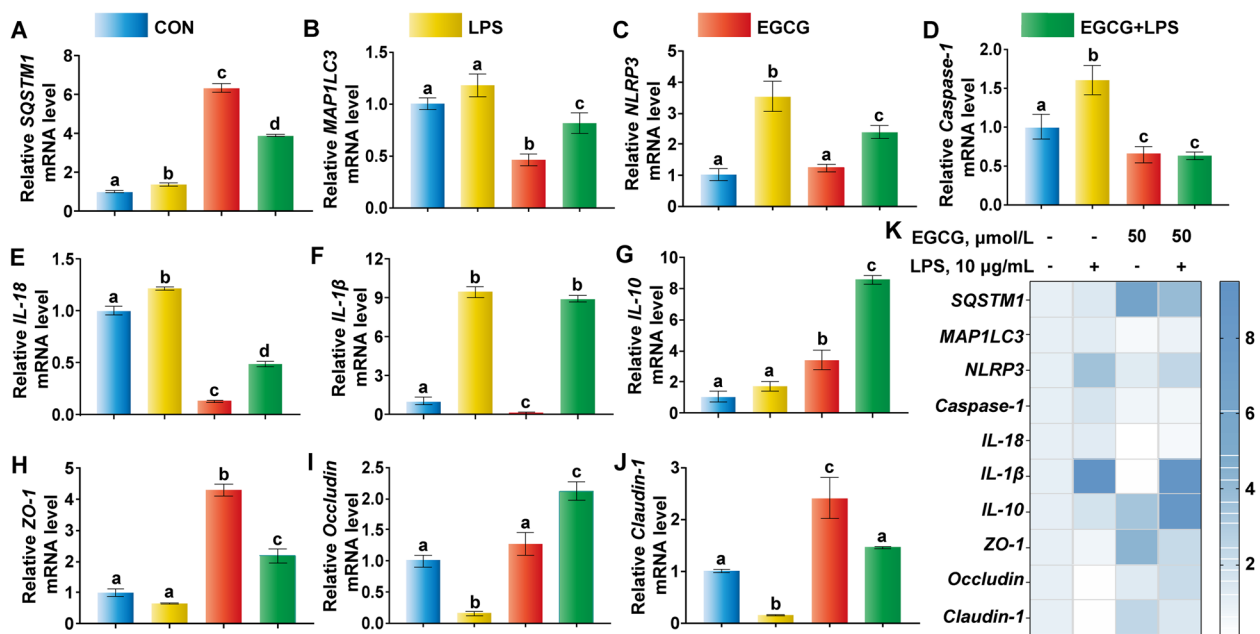


Fig. 6 Epigallocatechin-3-gallate (EGCG) activated autophagy and NLR family pyrin domain containing 3 (NLRP3) inflammasome-mediated signaling pathway base on the mRNA expression level. BREC were pre-treated with 50 μmol/L EGCG for 6 h and then added 10 μg/mL LPS for 6 h in 6-well plates (2.5 × 10⁶ cells/mL). **A–J** The mRNA abundance of Sequestosome 1 (SQSTM1), Microtubule-associated protein 1 light chain 3 (MAP1LC3), NLRP3, caspase-1, IL-18, IL-1β, IL-10, ZO-1, Occludin, Claudin-1. **K** Heat map analysis of the mRNA abundance. ^{a–d}Values without the same letters indicate a significant difference (*P* < 0.05)

ruminal epithelial barrier, in part due to inflammatory events that are often alleviated with the use of drugs or antibiotics [35]. Because polyphenols have been proven in a number of studies to control and alleviate inflammation [36–38], they could serve as alternatives to antibiotics as well. Our data further confirmed that SARA causes ruminal epithelium injury and systemic inflammation in vivo, and in vitro data revealed that EGCG protects BREC against LPS-induced inflammatory damage. The mechanism of action includes the activation of autophagy, thus, this polyphenol has the potential to be used as a therapeutic strategy for SARA-associated inflammation diseases. The cell viability assay via CCK8 also confirmed that at the dosages of LPS (10 μg/mL) and EGCG (10, 20 and 50 μmol/L) used in the present study there were no evident cytotoxic effects, thus, confirming the validity of the model to study the anti-inflammatory effects of EGCG.

The NLRP3 inflammasome is a multi-protein complex composed of the intracellular innate immune receptor NLRP3, the adaptor protein ASC, and the protease caspase-1 [39]. It recognizes DAMPs or PAMPs and recruits and activates the inflammatory protease caspase-1, and the latter cleaves the IL-1β and IL-18 precursors into their mature forms, thus, triggering an inflammatory response [40, 41]. The NLRP3 inflammasome can be activated by multiple exogenous and endogenous stimuli,

including pathogenic infections caused by bacteria, fungi, and viruses, as well as LPS [42]. However, the fact that EGCG in vitro (at 50 μmol/L) significantly suppressed the release of pro-inflammatory cytokines due to LPS-induction, by downregulating transcription of the cytokines and chemokines, strongly suggested that this compound could be of practical value as a therapeutic tool.

At least in ruminants, there has been uncertainty as to the molecular targets affected by EGCG that can play an anti-inflammatory effect. As such, it was essential to outline the major mechanism whereby LPS triggered inflammation in BREC before we could elucidate if EGCG participated in such pathway. The increased phosphorylation of IκBα and NF-κBp65 along with the translocation of NF-κBp65 to the nucleus in response to LPS confirmed that this molecule works through the canonical NF-κB pathway [43]. Thus, the negative effect of EGCG on the mRNA abundance of TLR4 signaling components, phosphorylation of IκBα, NF-κBp65, NLRP3 and caspase-1 protein abundance confirmed that EGCG elicit an anti-inflammatory response by preventing activation of the NF-κB pathway and NLRP3 inflammasome in ruminal epithelial cells.

Because of its potential to eliminate pathogens (xenophagy) and activate immunity while limiting excessive inflammation, autophagy can impact immunity and inflammation [44]. In non-ruminants, autophagy induced

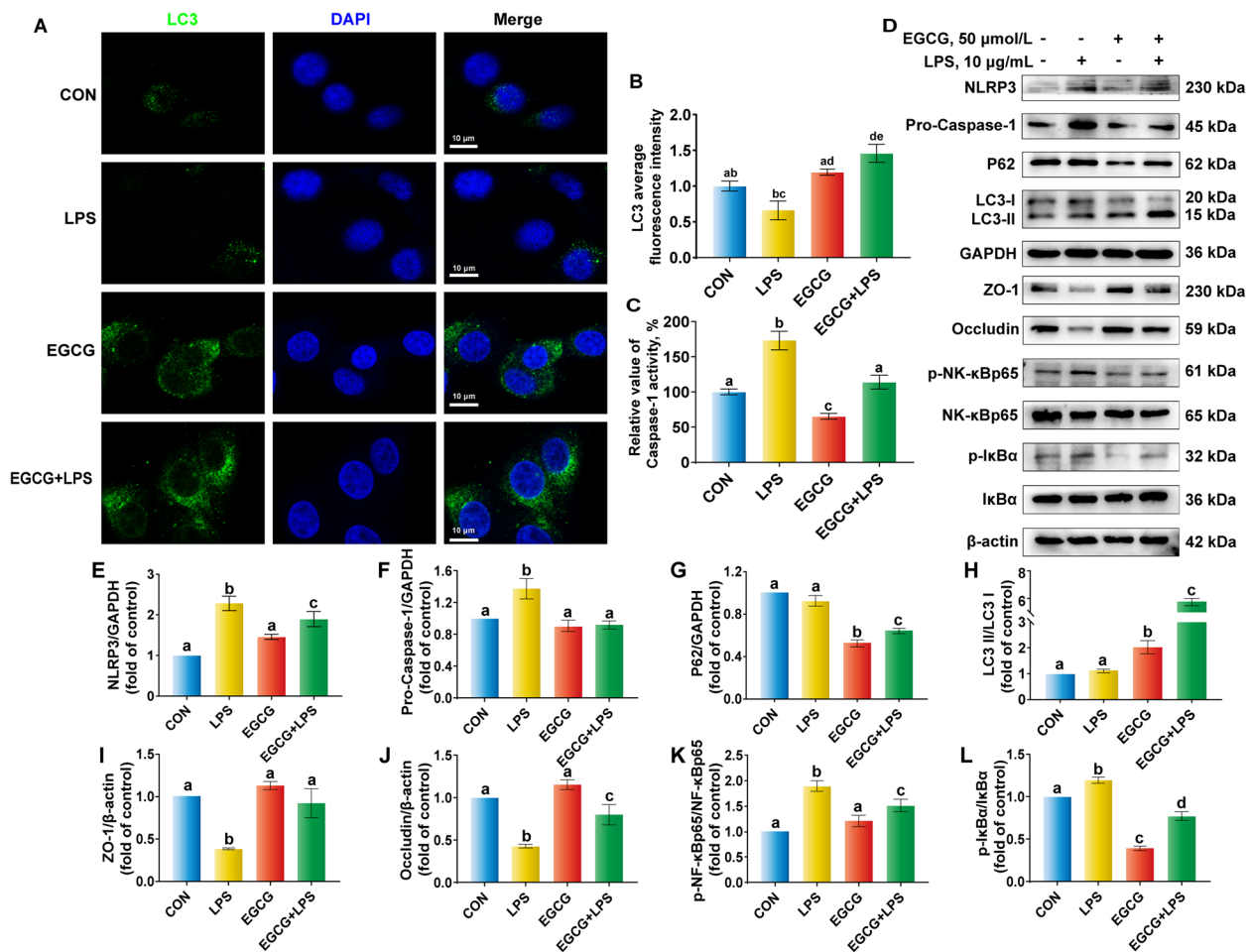


Fig. 7 Effect of epigallocatechin-3-gallate (EGCG) on autophagy activation and NLR family pyrin domain containing 3 (NLRP3) inflammasome-mediated signaling pathway in lipopolysaccharide (LPS)-challenged bovine ruminal epithelial cells (BREC). **A** and **B** Green light represents LC3 and blue light represents nucleus. Scale bar = 10 μm; Images are representative of three independent experiments. **C** Caspase-1 activity. **D–L** Western blot analysis of the abundance of NLRP3, pro-caspase-1, p62, LC3, ZO-1, Occludin, phosphorylated-nuclear factor kappa-B (p-NF-κB) p65, NF-κBp65, p-IκBα and IκBα^{a,b} Values without the same letters indicate a significant difference ($P < 0.05$)

by EGCG was implicated in the prevention of various human diseases such as cancer, diabetes, and cardiovascular disease [45]. In rats, exogenous EGCG also alleviated inflammatory responses by restoring autophagic flux via downregulation of Beclin1, Autophagy-related gene 5 (Atg5), and Sequestosome 1 (SQSTM1, p62) [46]. EGCG decreased dimerization of LC3B-I, enhanced LC3B-II synthesis, and activated autophagy in hepatocellular carcinoma cells [47]. The upregulation of LC3II and downregulation of p62 protein abundance (an autophagy adaptor responsible for autolysosome degradation) in response to EGCG and LPS indicated an increased in autophagic activity [48]. Together the data provide strong evidence for a link between EGCG and enhanced autophagy activation coupled with an anti-inflammatory response in the cellular response to LPS.

Non-ruminant studies over the last decades have reported that autophagy can regulate inflammasome activity, particularly NLRP3 inflammasome activation [18, 49, 50]. Our present data further confirmed that EGCG in ruminal epithelium can also reverse NLRP3-mediated caspase-1 activation and IL-1β release by activating autophagy. This was further confirmed by the inability of exogenous EGCG to activate autophagy when the BREC incubation contained the autophagy inhibitor chloroquine, i.e., both the anti-inflammatory response was reduced (NLRP3 inflammasome formation increased) and breakdown of tight junctions could not be prevented. The latter response is particularly important in the context of proper epithelial barrier function because maintenance of an intact intestinal barrier is crucial in preventing the translocation of intestinal

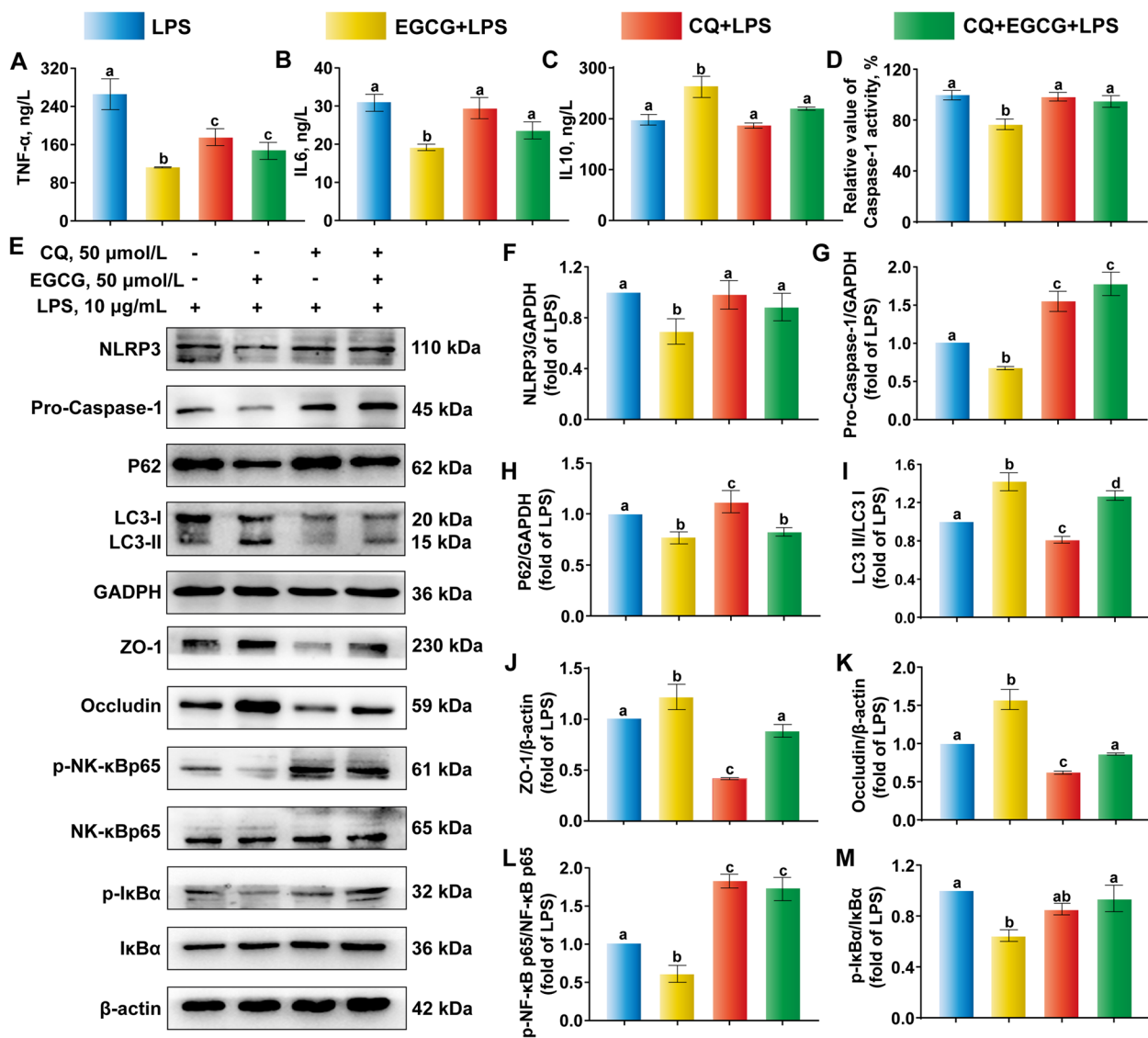


Fig. 8 Effects of autophagy inhibition on NLR family pyrin domain containing 3 (NLRP3) inflammasome-mediated signaling pathway. Bovine ruminal epithelial cells (BREC) were pre-treated with chloroquine (50 μ mol/L) for 4 h, followed by treated with epigallocatechin-3-gallate (EGCG) (50 μ mol/L) for 6 h and treated with lipopolysaccharide (LPS) (10 μ g/mL) for an additional 6 h. **A–D** The production of inflammatory cytokines of tumor necrosis factor (TNF- α), IL-6, IL-10 and the caspase-1 activity. **(E–M)** Western blot analysis of the expression of NLRP3, pro-caspase-1, p62, LC3, ZO-1, Occludin, phosphorylated-nuclear factor kappa-B (p-NF- κ B) p65, NF- κ Bp65, p-I κ B α and I κ B α . ^{a–d}Values without the same letters indicate a significant difference ($P < 0.05$)

bacteria, toxic substances, or allergens from the gut into the bloodstream [51].

In bovine, Gram-negative ruminal bacteria are the main source of LPS in the rumen [52]. Cows diagnosed with SARA often exhibit low pH levels and elevated concentrations of free LPS in the rumen, which if not treated properly can trigger a proinflammatory response [53, 54]. When the ruminal epithelium is inflamed, a decrease in barrier function increases the chance for pathogenic

substances, including LPS, to enter the blood circulation and negatively affect other organs such as the liver, udder and uterus [6, 7, 55]. The present in vitro data confirmed that LPS has a negative impact on TJ proteins such as ZO-1 and Occludin and that EGCG (10, 20 and 50 μ mol/L) can reverse this negative effect. Overall, the present data indicated that EGCG can act as a protective agent against LPS-induced ruminal epithelial cell inflammation and barrier injury.

Conclusions

Subacute ruminal acidosis (SARA) can induce ruminal epithelium damage and inflammation, which would enhance transport of inflammatory factors into the bloodstream and increase the risk of systemic inflammation. The inclusion of epigallocatechin-3-gallate (EGCG), a major catechin found in green tea, in the diet could aid in preventing these responses via inducing autophagy, preventing the NF- κ B inflammatory signaling pathway and formation of NLRP3 inflammasome. Further in vivo studies should be performed to confirm these findings.

Abbreviations

ACTB	β -Actin
AMPK	Adenosine 5'-monophosphate (AMP)-activated protein kinase
AP-1	Activator protein-1
ASC	Apoptosis-associated speck-like protein containing a CARD
ATG16L1	Autophagy-related protein 16-like 1
BREC	Bovine ruminal epithelial cells
CCK-8	Cell Counting Kit-8
COX	Cytochrome c oxidase
DAMPs	Danger-associated molecular patterns
EGCG	Epigallocatechin-3-gallate
GAPDH	Glyceraldehyde-3-phosphate dehydrogenase
IFN- β	Interferon- β
LPS	Lipopolysaccharides
MyD88	Myeloid differentiation primary response protein 88
NF- κ B	Nuclear factor kappa-B
NLRP3	NLR family pyrin domain containing 3
NO	Nitric oxide
PAMPs	Pathogen-associated molecular patterns
ROS	Reactive oxygen species
SARA	Subacute ruminal acidosis
TJ	Tight junction
TLR4	Toll-like receptor 4
TNF	Tumor necrosis factor

Supplementary Information

The online version contains supplementary material available at <https://doi.org/10.1186/s40104-024-01066-9>.

Additional file 1. Primer sequences used for quantitative real-time PCR.

Acknowledgements

Not applicable.

Authors' contributions

CX, TS, ZD, WZ designed the experiments. WZ performed the experiments. WZ, ML and YH analyzed the data. WZ, BZ, BA, JL and AP wrote and revised the manuscript. All authors reviewed and approved the final manuscript.

Funding

This work was supported by the National Natural Science Foundation of China (Beijing, China; grant nos. 32125038).

Availability of data and materials

All data generated or analyzed during this study are included in this published article. Further inquiries can be directed to the corresponding author.

Declarations

Ethics approval and consent to participate

Not applicable.

Consent for publication

Not applicable.

Competing interests

The authors declare no competing financial interests.

Author details

¹National Key Laboratory of Veterinary Public Health and Safety, College of Veterinary Medicine, China Agricultural University, 2 Yuanmingyuan West Road, Beijing 100193, China. ²Department of Biosystems, Division of Animal and Human Health Engineering, KU Leuven University, Kleinhofstraat 4, Geel 2440, Belgium. ³Department of Animal Sciences, Division of Nutritional Sciences, University of Illinois, Urbana-Champaign, Urbana, IL 61801, USA. ⁴Department of Clinical Science and Services, Queen Mother Hospital for Animals, The Royal Veterinary College, North Mymms, Hawkshead Lane, Hatfield, Hertfordshire AL9 7TA, UK.

Received: 20 April 2024 Accepted: 19 June 2024

Published online: 09 August 2024

References

- Nagaraja TG, Titgemeyer EC. Ruminal acidosis in beef cattle: the current microbiological and nutritional outlook. *J Dairy Sci.* 2007;90:E17-38. <https://doi.org/10.3168/jds.2006-478>.
- Simanungkalit G, Bhuiyan M, Bell R, Sweeting A, Morton CL, Cowley F, et al. The effects of antibiotic-free supplementation on the ruminal pH variability and methane emissions of beef cattle under the challenge of subacute ruminal acidosis (SARA). *Res Vet Sci.* 2023;160:30-8. <https://doi.org/10.1016/j.rvsc.2023.05.006>.
- Li S, Khafipour E, Krause DO, Kroeker A, Rodriguez-Lecompte JC, Gozho GN, et al. Effects of subacute ruminal acidosis challenges on fermentation and endotoxins in the rumen and hindgut of dairy cows. *J Dairy Sci.* 2012;95(1):294-303. <https://doi.org/10.3168/jds.2011-4447>.
- Zebeli Q, Ametaj BN. Relationships between rumen lipopolysaccharide and mediators of inflammatory response with milk fat production and efficiency in dairy cows. *J Dairy Sci.* 2009;92(8):3800-9. <https://doi.org/10.3168/jds.2009-2178>.
- Meissner S, Hagen F, Deiner C, Günzel D, Greco G, Shen Z, et al. Key role of short-chain fatty acids in epithelial barrier failure during ruminal acidosis. *J Dairy Sci.* 2017;100(8):6662-75. <https://doi.org/10.3168/jds.2016-12262>.
- Aschenbach JR, Zebeli Q, Patra AK, Greco G, Amasheh S, Penner GB. Symposium review: the importance of the ruminal epithelial barrier for a healthy and productive cow. *J Dairy Sci.* 2019;102(2):1866-82. <https://doi.org/10.3168/jds.2018-15243>.
- Plaizier JC, Khafipour E, Li S, Gozho GN, Krause DO. Subacute ruminal acidosis (SARA), endotoxins and health consequences. *Anim Feed Sci Technol.* 2012;172(1-2):9-21. <https://doi.org/10.1016/j.anifeedsci.2011.12.004>.
- Takeuchi O, Akira S. Pattern recognition receptors and inflammation. *Cell.* 2010;140(6):805-20. <https://doi.org/10.1016/j.cell.2010.01.022>.
- Negishi H, Fujita Y, Yanai H, Sakaguchi S, Ouyang X, Shinohara M, et al. Evidence for licensing of IFN- γ -induced IFN regulatory factor 1 transcription factor by MyD88 in Toll-like receptor-dependent gene induction program. *Proc Natl Acad Sci USA.* 2006;103(41):15136-41. <https://doi.org/10.1073/pnas.0607181103>.
- Zhan X, Li Q, Xu G, Xiao X, Bai Z. The mechanism of NLRP3 inflammasome activation and its pharmacological inhibitors. *Front Immunol.* 2023;13:1109938. <https://doi.org/10.3389/fimmu.2022.1109938>.
- Lasithiotaki I, Tsitoura E, Samara KD, Trachalaki A, Charalambous I, Tzanakis N, et al. NLRP3/Caspase-1 inflammasome activation is decreased in alveolar macrophages in patients with lung cancer. *PLoS One.* 2018;13(10):e0205242. <https://doi.org/10.1371/journal.pone.0205242>.
- Levine B. Autophagy and cancer. *Nature.* 2007;446(7137):745-7. <https://doi.org/10.1038/446745a>.
- Shintani T, Klionsky DJ. Autophagy in health and disease: a double-edged sword. *Science.* 2004;306(5698):990-5. <https://doi.org/10.1126/science.1099993>.

14. Mizushima N, Yoshimori T, Ohsumi Y. The role of Atg proteins in autophagosome formation. *Annu Rev Cell Dev Biol.* 2011;27(1):107–32. <https://doi.org/10.1146/annurev-cellbio-092910-154005>.
15. Zhong Y, Wang QJ, Li X, Yan Y, Backer JM, Chait BT, et al. Distinct regulation of autophagic activity by Atg14L and Rubicon associated with Beclin 1–phosphatidylinositol-3-kinase complex. *Nat Cell Biol.* 2009;11(4):468–76. <https://doi.org/10.1038/ncb1854>.
16. Mazure NM, Pouyssegur J. Hypoxia-induced autophagy: cell death or cell survival? *Curr Opin Cell Biol.* 2010;22(2):177–80. <https://doi.org/10.1016/j.ceb.2009.11.015>.
17. Tsvetkov AS, Miller J, Arrasate M, Wong JS, Pleiss MA, Finkbeiner S. A small-molecule scaffold induces autophagy in primary neurons and protects against toxicity in a Huntington disease model. *Proc Natl Acad Sci USA.* 2010;107(39):16982–7. <https://doi.org/10.1073/pnas.1004498107>.
18. Saitoh T, Akira S. Regulation of inflammasomes by autophagy. *J Allergy Clin Immunol.* 2016;138(1):28–36. <https://doi.org/10.1016/j.jaci.2016.05.009>.
19. Saitoh T, Fujita N, Jang MH, Uematsu S, Yang BG, Satoh T, et al. Loss of the autophagy protein Atg16L1 enhances endotoxin-induced IL-1 β production. *Nature.* 2008;456(7219):264–8. <https://doi.org/10.1038/nature07383>.
20. Wu Y, Tang L, Wang B, Sun Q, Zhao P, Li W. The role of autophagy in maintaining intestinal mucosal barrier. *J Cell Physiol.* 2019;234(11):19406–19. <https://doi.org/10.1002/jcp.28722>.
21. Nighot PK, Hu CAA, Ma TY. Autophagy enhances intestinal epithelial tight junction barrier function by targeting claudin-2 protein degradation. *J Biol Chem.* 2015;290(11):7234–7246. <https://doi.org/10.1074/jbc.M114.597492>.
22. Song JY, Han JH, Song Y, Lee JH, Choi SY, Park YM. Epigallocatechin-3-gallate can prevent type 2 human papillomavirus E7 from suppressing interferon-stimulated genes. *Int J Mol Sci.* 2021;22(5):2418. <https://doi.org/10.3390/ijms22052418>.
23. Zhou M, Dong J, Huang J, Ye W, Zheng Z, Huang K, et al. Chitosan-Gelatin-EGCG nanoparticle-mediated LncRNA TMEM44-AS1 silencing to activate the P53 signaling pathway for the synergistic reversal of 5-FU resistance in gastric cancer. *Adv Sci.* 2022;9(22):2105077. <https://doi.org/10.1002/advsc.202105077>.
24. Tao L, Forester SC, Lambert JD. The role of the mitochondrial oxidative stress in the cytotoxic effects of the green tea catechin, (–)-epigallocatechin-3-gallate, in oral cells. *Mol Nutr Food Res.* 2014;58(4):665–76. <https://doi.org/10.1002/mnfr.201300427>.
25. Kim JE, Kim TH, Kang TC. EGCG attenuates CA1 neuronal death by regulating GPx1, NF- κ B 536 phosphorylation and mitochondrial dynamics in the rat hippocampus following status epilepticus. *Antioxidants.* 2023;12(4):966. <https://doi.org/10.3390/antiox12040966>.
26. Kim SR, Seong KJ, Kim WJ, Jung JY. Epigallocatechin gallate protects against hypoxia-induced inflammation in microglia via NF- κ B suppression and Nrf-2/HO-1 activation. *Int J Mol Sci.* 2022;23(7):4004. <https://doi.org/10.3390/ijms23074004>.
27. Huang YJ, Wang KL, Chen HY, Chiang YF, Hsia SM. Protective effects of epigallocatechin gallate (EGCG) on endometrial, breast, and ovarian cancers. *Biomolecules.* 2020;10(11):1481. <https://doi.org/10.3390/biom10111481>.
28. Li W, Zhu S, Li J, Assa A, Jundoria A, Xu J, et al. EGCG stimulates autophagy and reduces cytoplasmic HMGB1 levels in endotoxin-stimulated macrophages. *Biochem Pharmacol.* 2011;81(9):1152–63. <https://doi.org/10.1016/j.bcp.2011.02.015>.
29. Kim H-S, Montana V, Jang H-J, Parpura V, Kim J. Epigallocatechin gallate (EGCG) stimulates autophagy in vascular endothelial cells: a potential role for reducing lipid accumulation. *J Biol Chem.* 2013;288(31):22693–705. <https://doi.org/10.1074/jbc.M113.477505>.
30. Zhou J, Farah BL, Sinha RA, Wu Y, Singh BK, Bay BH, et al. Epigallocatechin-3-gallate (EGCG), a green tea polyphenol, stimulates hepatic autophagy and lipid clearance. *PLoS One.* 2014;9(1):e87161. <https://doi.org/10.1371/journal.pone.0087161>.
31. Holczer M, Besze B, Zámbo V, Csala M, Bánhegyi G, Kapuy O. Epigallocatechin-3-Gallate (EGCG) promotes autophagy-dependent survival via influencing the balance of mTOR-AMPK pathways upon endoplasmic reticulum stress. *Oxid Med Cell Longev.* 2018;2018:6721530. <https://doi.org/10.1155/2018/6721530>.
32. Mu YY, Qi WP, Zhang T, Zhang JY, Mao SY. Gene function adjustment for carbohydrate metabolism and enrichment of rumen microbiota with antibiotic resistance genes during subacute rumen acidosis induced by a high-grain diet in lactating dairy cows. *J Dairy Sci.* 2021;104(2):2087–105.
33. Zhan K, Gong X, Chen Y, Jiang M, Yang T, Zhao G. Short-chain fatty acids regulate the immune responses via G protein-coupled receptor 41 in bovine rumen epithelial cells. *Front Immunol.* 2019;10:2042. <https://doi.org/10.3389/fimmu.2019.02042>.
34. Livak KJ, Schmittgen TD. Analysis of relative gene expression data using real-time quantitative PCR and the 2^{- Δ ACT} method. *Methods.* 2001;25(4):402–8. <https://doi.org/10.1006/meth.2001.1262>.
35. Plaizier JC, Danesh Mesgaran M, Derakhshani H, Golder H, Khafipour E, Kleen JL, et al. Review: enhancing gastrointestinal health in dairy cows. *Animal.* 2018;12:s399–418. <https://doi.org/10.1017/S1751731118001921>.
36. Tomás-Barberán FA, Andrés-Lacueva C. Polyphenols and health: current state and progress. *J Agric Food Chem.* 2012;60(36):8773–5. <https://doi.org/10.1021/jf300671j>.
37. Basiricò L, Morera P, Dipasquale D, Bernini R, Santi L, Romani A, et al. (–)-Epigallocatechin-3-gallate and hydroxytyrosol improved antioxidative and anti-inflammatory responses in bovine mammary epithelial cells. *Animal.* 2019;13(12):2847–56. <https://doi.org/10.1017/S1751731119001356>.
38. Wu Z, Huang S, Li T, Li N, Han D, Zhang B, et al. Gut microbiota from green tea polyphenol-dosed mice improves intestinal epithelial homeostasis and ameliorates experimental colitis. *Microbiome.* 2021;9:184. <https://doi.org/10.1186/s40168-021-01115-9>.
39. Kim YG, Kim SM, Kim KP, Lee SH, Moon JY. The role of inflammasome-dependent and inflammasome-independent NLRP3 in the kidney. *Cells.* 2019;8(11):1389. <https://doi.org/10.3390/cells8111389>.
40. Kelley N, Jeltema D, Duan Y, He Y. The NLRP3 inflammasome: an overview of mechanisms of activation and regulation. *Int J Mol Sci.* 2019;20(13):3328. <https://doi.org/10.3390/ijms20133328>.
41. Huang Y, Xu W, Zhou R. NLRP3 inflammasome activation and cell death. *Cell Mol Immunol.* 2021;18(9):2114–27. <https://doi.org/10.1038/s41423-021-00740-6>.
42. Li W, Cao T, Luo C, Cai J, Zhou X, Xiao X, et al. Crosstalk between ER stress, NLRP3 inflammasome, and inflammation. *Appl Microbiol Biotechnol.* 2020;104(14):6129–40. <https://doi.org/10.1007/s00253-020-10614-y>.
43. Zhao Y, Jaber VR, Pogue AI, Sharfman NM, Taylor C, Lukiw WJ. Lipopolysaccharides (LPS) as potent neurotoxic glycolipids in Alzheimer’s Disease (AD). *Int J Mol Sci.* 2022;23(20):12671. <https://doi.org/10.3390/ijms232012671>.
44. Deretic V, Levine B. Autophagy balances inflammation in innate immunity. *Autophagy.* 2018;14(2):243–51. <https://doi.org/10.1080/15548627.2017.1402992>.
45. Zhang S, Cao M, Fang F. The role of epigallocatechin-3-Gallate in autophagy and endoplasmic reticulum stress (ERS)-induced apoptosis of human diseases. *Med Sci Monit.* 2020;26. <https://doi.org/10.12659/MSM.924558>.
46. Xuan F, Jian J. Epigallocatechin gallate exerts protective effects against myocardial ischemia/reperfusion injury through the PI3K/Akt pathway-mediated inhibition of apoptosis and the restoration of the autophagic flux. *Int J Mol Med.* 2016;38(11):328–36. <https://doi.org/10.3892/ijmm.2016.2615>.
47. Zhao L, Liu S, Xu J, Li W, Duan G, Wang H, et al. A new molecular mechanism underlying the EGCG-mediated autophagic modulation of AFP in HepG2 cells. *Cell Death Dis.* 2017;8(11):e3160–e3160. <https://doi.org/10.1038/cddis.2017.563>.
48. Chao X, Wang S, Fulte S, Ma X, Ahamed F, Cui W, et al. Hepatocytic p62 suppresses ductular reaction and tumorigenesis in mouse livers with mTORC1 activation and defective autophagy. *J Hepatol.* 2022;76(3):639–51. <https://doi.org/10.1016/j.jhep.2021.10.014>.
49. Pang Q, Wang P, Pan Y, Dong X, Zhou T, Song X, et al. Irisin protects against vascular calcification by activating autophagy and inhibiting NLRP3-mediated vascular smooth muscle cell pyroptosis in chronic kidney disease. *Cell Death Dis.* 2022;13(3):283. <https://doi.org/10.1038/s41419-022-04735-7>.
50. Han X, Sun S, Sun Y, Song Q, Zhu J, Song N, et al. Small molecule-driven NLRP3 inflammation inhibition via interplay between ubiquitination and autophagy: implications for Parkinson disease. *Autophagy.* 2019;15(11):1860–81. <https://doi.org/10.1080/15548627.2019.1596481>.
51. Van Spaendonck H, Ceuleers H, Witters L, Patteet E, Joossens J, Augustyns K, et al. Regulation of intestinal permeability: the role of proteases. *World*

- J Gastroenterol. 2017;23(12):2106. <https://doi.org/10.3748/wjg.v23.i12.2106>.
52. Nagaraja TG, Lechtenberg KF. Acidosis in feedlot cattle. *Vet Clin North Am Food Anim Pract.* 2007;23(2):333–50. <https://doi.org/10.1016/j.cvfa.2007.04.002>.
 53. Zhao C, Liu G, Li X, Guan Y, Wang Y, Yuan X, et al. Inflammatory mechanism of rumenitis in dairy cows with subacute ruminal acidosis. *BMC Vet Res.* 2018;14:135. <https://doi.org/10.1186/s12917-018-1463-7>.
 54. Gozho GN, Krause DO, Plaizier JC. Rumen lipopolysaccharide and inflammation during grain adaptation and subacute ruminal acidosis in steers. *J Dairy Sci.* 2006;89(11):4404–13. [https://doi.org/10.3168/jds.S0022-0302\(06\)72487-0](https://doi.org/10.3168/jds.S0022-0302(06)72487-0).
 55. Zeng J, Lv J, Duan H, Yang S, Wu J, Yan Z, et al. Subacute ruminal acidosis as a potential factor that induces endometrium injury in sheep. *Int J Mol Sci.* 2023;24(2):1192. <https://doi.org/10.3390/ijms24021192>.